BIOCHEMISTRY
including biophysical chemistry & molecular biology

ARTICLE

pubs.acs.org/biochemistry

Nuclear Magnetic Resonance Solution Structures of Inter- and Intrastrand Adducts of DNA Cross-Linker SJG-136

Suzanne R. Hopton and Andrew S. Thompson*

Department of Pharmacy and Pharmacology, University of Bath, Claverton Down, Bath, England BA2 7AY

Supporting Information

ABSTRACT: SJG-136 (**1**) is a sequence-selective DNA-interactive agent that is about to enter phase II clinical trials for the treatment of malignant disease. Previous studies on the pyrrolo[2,1-*c*][1,4]benzodiazepine (PBD) dimers, typified by SJG-136 and DSB-120 (**2**), have shown that these planar ligands react with the exocyclic NH_2 groups of two guanine bases in the base of the minor groove of DNA to form an irreversible interstrand cross-linked sequence-specific adduct. Using high-field NMR, we have characterized and modeled the previously predicted interstrand duplex adduct formed by SJG-136 with the self-complementary 5′-d(CICGATCICG)$_2$ duplex (**4**). This first SJG-136 NMR-refined adduct structure has been compared with previous high-field NMR studies of the adducts of the closely related PBD dimer DSB-120 with the same duplex and of the adduct of tomaymycin (**3**) formed with 5′-d(ATGCAT)$_2$. Surprisingly, the SJG-136 duplex adduct appears to be more closely related to the tomaymycin adduct than to the DSB-120 adduct with respect of the orientation and depth of insertion of the ligand within the minor groove. The intrastrand duplex adduct formed in the reaction of SJG-136 with the noncomplementary 5′-d(CTCATCAC)·(GTGATGAG) duplex (**5**) has also been synthesized and modeled. In this duplex adduct, the nature of the cross-link was confirmed, the central guanines were identified as the sites of alkylation, and the stereochemical configuration at C11 at both ends of the SJG-136 molecule was determined to be *S*. The NMR-refined solution structures produced for the intrastrand adduct confirm the previously proposed structure (which was based solely on mass spectroscopy). Both the inter- and intrastrand SJG-136 duplex adducts form with minimal distortion of the DNA duplex. These observations have an impact on the proposal for the mechanism of action of SJG-136 both in vitro and in vivo, on the repair of its adducts and mechanism of resistance in cells, and, potentially, on the type of pharmacodynamic assay to be used in clinical trials. SGJ-136 is currently in phase II clinical trials with several groups working on both dimeric cross-linking agents and monoalkylating ligands based on the PBD alkylating moiety. This study suggests subtle differences between the DNA binding of SJG-136 and the C2 unsubstituted analogue DSB-120 that are likely to be the origins of the differences in potency. Confirmation of the stereochemical configuration at the C11 position (particularly in the intrastrand adduct) provides confirmation of binding orientation that was previously only speculation in the HPLC MS study. Together, these observations are likely to be of value in the development of third-generation PBD-based cross-linkers and monoalkylating analogues.

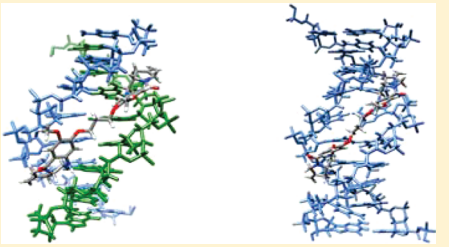

The pyrrolo[2,1-*c*][1,4]benzodiazepines (PBDs) make up a family of naturally occurring antitumor antibiotics produced by various *Streptomyces* species.[1] The naturally occurring and synthetic monomers exert their biological activity by reacting covalently with the exocyclic NH_2 group of guanine within the minor groove of DNA with sequence specificity for 5′-purine-guanine-purine sequences.[2] PBD dimers were designed and synthesized by joining two PBD subunits via flexible linkers; initial studies used molecules that were connected from either the C8[3−7] or C7[8] position on the aromatic ring. The C8 dimers typified by DSB-120 and SJG-136 (Figure 1) have been shown previously to form nondistorting interstrand cross-links within the minor groove of DNA and have significantly higher cytotoxicity than the monofunctional PBDs.[9] SJG-136 (SG2000) has recently completed phase I clinical trials in the United Kingdom[10] and United States[11,12] and is about to enter phase II evaluation against both solid tumors and hematologic malignancies.[13]

The structures of PBD−DNA duplex adducts (both monomers and dimeric analogues) have been the subject of many studies, including NMR,[14−16] X-ray crystallography,[17] molecular modeling,[18,19] and gel electrophoresis.[20,21] More recent mass spectroscopic studies have shown that the PBD dimer SJG-136 is able to form both inter- and intra-strand cross-linked duplex adducts.[22,23] However, until these MS studies, only the interstrand adducts had been observed and reported. This is primarily due to limitations in the techniques, mainly DNA footprinting, melting, and cross-linking assays, used to study the DNA interactions and confusion with possible monoalkylation products and/or interstrand cross-linking interactions. Previous NMR studies with the dimeric PBDs were conducted with DSB-120 and, although the binding was assumed to be the same for SJG-136, significant differences exist in terms of DNA interactions and in vitro cytotoxicity.

Received: December 20, 2010
Revised: April 8, 2011
Published: April 13, 2011

ACS Publications © 2011 American Chemical Society

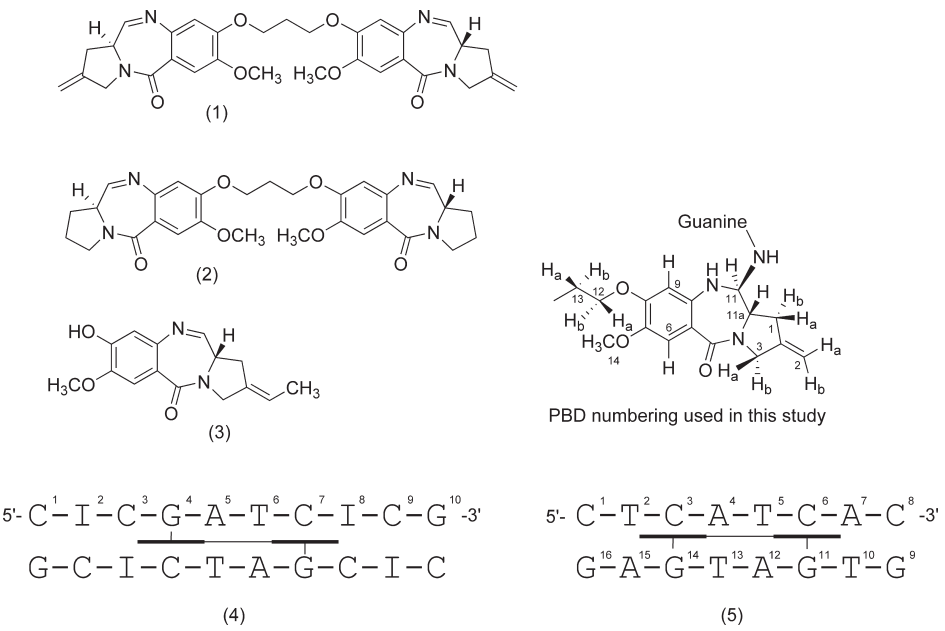

Figure 1. Structures of SJG-136 (**1**), DSB-120 (**2**), tomaymycin (**3**), and the interstrand (**4**) and intrastrand (**5**) duplex adducts showing base pair numbering used in this study.

In this study, we compare the binding of SJG-136 to DNA with the binding of the preferred interstrand cross-link site 5′-GATC-3′ to the previous DSB-120 study,[24] also comparing this to a previous NMR study of tomaymycin. We also report the first NMR-based structure for the intrastrand duplex adducts confirming the nature and sites of alkylation, the stereochemical configuration at C11, and the location of the SJG-136 ligand within the minor groove. These results provide significant insight into the nature of these interactions and suggest opportunities for future drug design.

EXPERIMENTAL PROCEDURES

Chemicals. SJG-136 was a gift from Ipsen Pharmaceuticals (Paris, France) and was used without additional purification. Reagents used to prepare the NMR buffers, sodium hydrogen phosphate (99.99%), sodium chloride (99.99%), and EDTA (99.99%), were purchased from Aldrich. HPLC grade acetonitrile, acetic acid, and methanol were purchased from Aldrich. Reagents and solvents for automated DNA synthesis were purchased from Applied Biosystems/Cruachem. DNA-grade Bio-Gel hydroxyapatite was purchased from Bio-Rad.

Preparation of Oligonucleotides and Purification for NMR Studies. The single strand for the self-complementary intrastrand adduct duplex 5′-d(CICGATCICG)$_2$ and the two strands for the 5′-d(CTCATCAC)·(GTGATGAG) duplex were synthesized on a 2 × 15 μmol scale using automated solid-phase phosphotriester and phosphoramidite chemistry[25] on an Applied Biosystems automated DNA synthesizer (model 381A), leaving the trityl protecting group on each of the strands. Each strand was deprotected overnight in saturated aqueous ammonia, followed by purification by reversed-phase HPLC, as outlined previously.[26] The DNA was detritylated using 50% aqueous acetic acid, and the solvents were evaporated, followed by further purification by HPLC. The self-complementary 5′-d(CICGATCICG)$_2$ sample was desalted (dialysis) and then annealed in NMR buffer [10 mM NaH_2PO_4, 100 mM NaCl, and 0.1 mM EDTA (pH 6.85)]; only duplex signals were observed in the ^{1}H NMR spectrum. The two strands for the 5′-d(CTCATCAC)·(GTGATGAG) duplex were desalted (dialysis) and dissolved in NMR buffer [10 mM NaH_2PO_4, 100 mM NaCl, and 0.1 mM EDTA (pH 6.85)]. Proton NMR spectra of the two purified DNA strands were recorded. Approximately 90% of the two were mixed together (based on the signal-to-noise ratio in the ^{1}H NMR spectrum) and annealed by slow cooling from 80 °C to give the designed duplex. An observed slight excess of one strand was addressed by adding a small amount of the second strand to produce the duplex with no trace of either of its component single DNA strands. This duplex was then desalted (dialysis) and redissolved in NMR buffer [10 mM NaH_2PO_4, 100 mM NaCl, and 0.1 mM EDTA (pH 6.85)] to give the final DNA duplex sample (full NMR assignment was conducted on the duplexes prior to formation of the adducts).

Preparation of Adducts and Purification for NMR Studies. The SJG-136 adducts were prepared by stirring SJG-136 (5 mg) in deuterated DMF (0.2 mL) with 30 μmol of the purified duplexes in twice-concentrated deuterated NMR buffer (pH 6.85, 500 μL). The reactions were followed by ^{1}H NMR spectroscopy; after 16 h at 5 °C, none of the duplex signals could be observed in either sample and a new set of signals arising from the adduct was present. Previous MS studies[23] noted a significant difference in the reaction times for the formation of the inter- and intrastrand duplex adducts with the interstrand adduct forming in 5 min compared to 12 h for the intrastrand adduct. One-dimensional ^{1}H NMR data collected over the first few hours indicated that the two duplex adducts studied here also reacted at different rates, with the interstrand adduct forming significantly more quickly. However, because neither sample had completely reacted after 2 h, we decided to place both in a cool room overnight (16 h), after which both adducts had completely formed. The poor solubility of the SJG-136 and suspension formed in the reaction mixture coupled with the use of DMF as a cosolvent makes accurate study of the reaction mixtures difficult. However, within both data sets, it appeared that transient intermediate species are formed (possible monoalkylation products) before the final adducts are produced.

dx.doi.org/10.1021/bi102017e |*Biochemistry* 2011, 50, 4720–4732

The samples were lyophilized to remove the solvent and cosolvent and resuspended in D_2O (500 μL). One-dimensional ^1H NMR now revealed only duplex adduct signals. The sample was again lyophilized to dryness and desalted. Excess drug was then removed on C18 Sep-Pak cartridges, and the sample was lyophilized to dryness and redissolved in deuterated NMR buffer.

Proton NMR Experiments. One- and two-dimensional 600 MHz NMR data sets were recorded in buffered solutions in H_2O and D_2O on a Varian Inova 600 (600 MHz) spectrometer. Proton signals were recorded in parts per million and referenced relative to the residual water signal (δ 4.71). Phase-sensitive two-dimensional NOESY spectra (Varian) were recorded with mixing times of 50, 100, 200, and 300 ms, with 32 scans at each of 1024 t_1 values at a spectral width of 10.002 ppm with a relaxation delay of 2.0 s between scans. Two-dimensional NOE spectra in 90% H_2O with mixing times of 150 and 300 ms were recorded; HDO suppression was achieved by using Varian presaturation suppression or a 1-1 echo read pulse sequence[27,28] with a 1.5 s pulse repetition delay and a sweep width of 25 ppm. Spectra were processed on the Inova spectrometer (VNMR 6.1c) and also in the TRIAD module of the SYBYL software suite. During data processing, a 90°-shifted sine-bell function was used in the F_1 and F_2 dimensions. The FID in F_1 was zero-filled to 2K prior to FT to give a 2K × 2K spectrum. DQF-COSY, TOCSY, and ROESY spectra were also recorded with the Varian 600 MHz spectrometer and were used to confirm assignments made in the NOESY spectra. In addition, selected ^{13}C resonances were identified using a heteronuclear multiple-quantum coherence experiment in D_2O.[29]

Molecular Modeling. Additional base pairs (G-C) were added to the top and bottom of the duplexes to give a dodecamer; this approach significantly reduced the likelihood of terminal base pairs fraying within the calculations and kept the central octamer free from artificial restraints. The DNA duplexes were built using the Bio Polymer module of SYBYL, and the SJG-136 ligand was docked and bound into the minor groove. Charges were then calculated for the complete complexes using the Gasteiger−Hückel set of charges.[30,31] Counterions were placed on the O−P−O bisector 6.0 Å from the phosphorus atom prior to solvation.[32] The systems were solvated as a droplet using six layers of solvent using the Molecular Silverware algorithm.[33]

Restrained Molecular Mechanics and Dynamics Simulations. Interproton distance constraints were generated from the NOESY data in TRIAD and were incorporated into the adduct model using a weak, medium, and strong methodology.[34,35] Distance restraints were primarily taken from 50 and 100 ms NOESY data sets and were distributed according to cross-peak intensities as strong (1.75−2.90 Å), medium (2.00−3.50 Å), and weak (2.25−4.00 Å) additional restraints were added from a 300 ms NOESY data set (NOEs not observed in 50 or 100 ms data sets) and placed at 3.00−4.50 Å. In total, <1% of the NOE data was not observed within the short mixing time data sets and, with such a broad range, the NOE distance restraints from the 300 ms data set will not significantly affect the model; however, incorporating them allowed us to monitor and confirm assignments. Distance restraints from exchangeable protons were incorporated with distance constraints of 1.75−4.5 Å to avoid errors resulting from water suppression. The decision to use the weak, medium, and strong methodology was based on the complexity of the spectra and the difficulty in obtaining clean NOE volume data particularly within the non-self-complementary intrastrand duplex adduct. Although this approach will lead to the development of spin diffusion artifacts in NOE NMR data at long mixing times, the vast majority of the NOE distance restraints came for the 50 and 100 ms NOESY spectra where spin diffusion artifacts were less likely to be an issue. In many cases, the NOE signals were partially overlapped and the weak, medium, and strong approach used within this study allowed manual estimation of the contribution to the NOE peaks. The direct spin−spin systems (C1 H5−C1 H6 and C9 H5−C9 H6) were used to provide an internal reference. The rMD calculations were performed using the Tripos Associates force fields within the SYBYL software suite on Intel quad core workstations (SUSE LINUX). The molecular dynamics calculations (in aquo) were performed at a constant volume, using 2.0 fs time steps. The equilibrium protocol consisted of 100 steps of steepest descent minimization, followed by conjugate gradient minimization, applied to the solvent molecules to relax possible steric clashes at the adduct−solvent interface.[35] The water was then thermalized at 300 K for 5.0 ps using a Boltzman initial velocity distribution, a constant dielectric function, and fixed DNA with counterions. Finally, the molecular dynamics simulation was performed with only the DNA fixed, with the counterions and water mobilized at 300 K for 5.0 ps. The rMD calculations on the complete solvated complex were started at 0 K and ramped over 50 ps in 10 steps to 300 K. Alternative starting structures were (a) SJG-136 12-mer nonrestrained molecular dynamics products and (b) minimized B-DNA adducts. For the self-complementary intrastrand adduct, during the first 50 ps, the 185 NMR-derived distance restraints (46 of which were related to the bound SJG-136 (Table 2) were applied to the system along with additional distance restraints, which were applied between the base pairs and to the counterions. During the next 5.0 ps, the non-NMR-derived distance restraints were removed from all but the two 5′- and 3′-terminal bases (G-C), which were left in place to prevent the duplex from fraying at elevated temperatures. The non-self-complementary interstrand adduct was treated the same way (290 NMR-derived distance restraints, 70 of which were related to the bound SJG-136). The in vacuo and solvated systems were then held at 300 K for 60 ps, and the data from the last 50 ps (501 structures) were averaged and minimized to generate the averaged in vacuo and solvated structures.

RESULTS

5′-d(CICGATCICG)$_2$−SJG-136 Interstrand Adduct. The duplex used in this study is identical to the duplex used in the previous study of DSB-120,[24] which allows direct comparisons to be made. The resonances were assigned by two-dimensional NMR spectra employing through-bond COSY and through-space NOESY connectivities. The expansion of the H6/H8−H1′ region of the adduct NOESY spectrum can be seen in Figure 2. The chemical shift assignments for the nucleotide and drug protons in the duplex and adduct are listed in Table 1. There were no duplex resonances remaining after reaction with SJG-136, confirming that the reaction had proceeded to completion. Four strong COSY peaks can be identified within the aromatic protons concurrent with the cytosine H5−cytosine H6 interaction of the four cytosine peaks. This confirms that the self-complementary nature of the duplex has been retained, an observation that is supported by the presence of a single proton walk in the H6/H8−H1′ region (along with other aromatic H6/H8−H3′ and −H2′/H2″ associated walks).

Identification of the Covalent Linkage Site. PBD ligands are known to exist in equilibrating carbinolamine and imine forms.

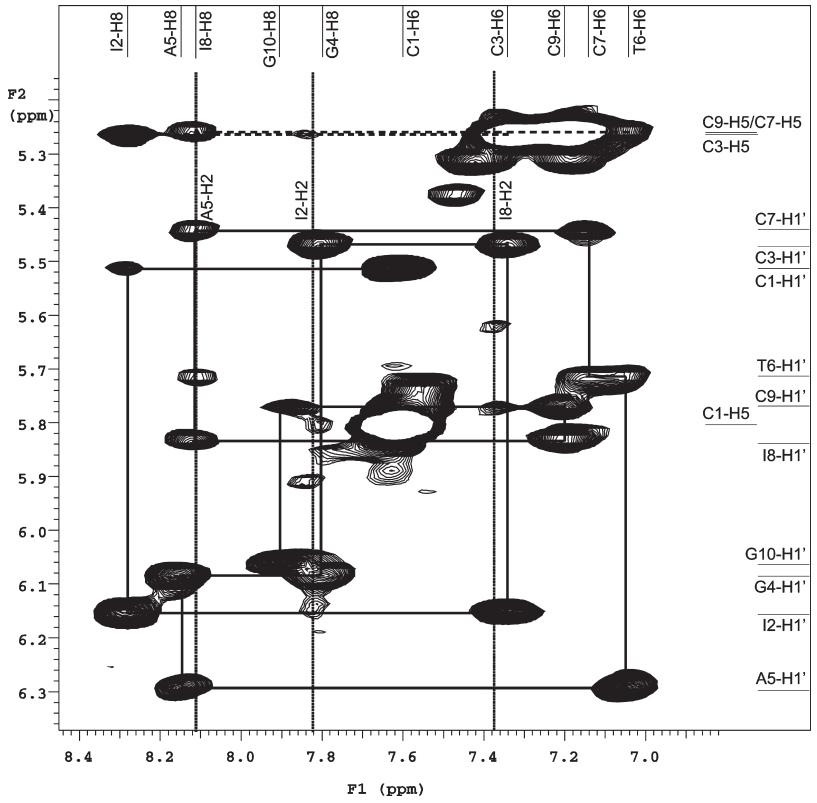

Figure 2. Two-dimensional phase-sensitive NOESY spectrum (200 ms mixing time) expanded contour plot of the SJG-136 interstrand cross-linked duplex adduct in buffered D_2O solution (pH 6.75) at 300 K, displaying connectivities from aromatic PuH8/PyH6 to deoxyribose H1′ and deoxyribose H1′ of the 5′-neighbor.

Table 1. Chemical Shifts of 5′-d(CICGATCICG)$_2$ Duplex and 5′-d(CICGATCICG)$_2$−SJG-136 Adduct DNA Protons

	H8/H6			H1′			H2′			H2″			H3′			H4′			H5/CH$_3$/H2		
	duplex	adduct		duplex	adduct		duplex	adduct		duplex	adduct		duplex	adduct		duplex	adduct		duplex	adduct	
C1	7.69	7.60	0.09	5.56	5.52	0.04	1.90	1.82	0.02	2.30	2.28	0.02	4.63	4.61	0.02	3.64	3.63	0.01	5.85	5.80	0.05
I2	8.39	8.28	0.11	6.11	6.15	0.04	2.71	2.66	0.05	2.82	2.82	0.00	4.95	4.91	0.04	4.34	4.32	0.02	7.92	7.82	0.10
C3	7.28	7.34	0.06	5.70	5.47	0.23	1.68	1.86	0.18	2.23	2.27	0.04	4.75	4.92	0.17	4.03	4.06	0.03	5.24	5.26	0.02
G4	7.94	7.80	0.14	5.49	6.08	0.06	2.66	2.66	0.00	2.71	2.94	0.23	4.93	4.95	0.02	4.30	4.06	0.24	–	–	–
A5	8.20	8.15	0.05	6.14	6.30	0.16	2.71	2.46	0.25	2.84	2.66	0.18	4.90	4.88	0.02	4.16	3.94	0.22	7.76	8.11	0.35
T6	7.17	7.05	0.12	5.80	5.71	0.09	1.94	1.94	0.00	2.37	2.17	0.20	4.77	4.55	0.22	4.20	3.98	0.22	1.23	1.20	0.02
C7	7.53	7.14	0.39	5.48	5.44	0.04	2.00	2.09	0.09	2.32	1.65	0.67	4.95	4.71	0.24	4.05	4.02	0.03	5.52	5.26	0.26
I8	8.33	8.12	0.21	6.08	5.84	0.24	2.64	2.57	0.07	2.80	2.10	0.70	4.94	4.83	0.11	4.06	3.82	0.24	7.72	7.38	0.34
C9	7.28	7.20	0.08	5.76	5.77	0.02	1.58	1.46	0.12	2.15	2.13	0.02	4.92	4.71	0.21	3.99	3.94	0.05	5.30	5.26	0.04
G10	7.96	7.90	0.06	6.05	6.06	0.01	2.28	2.26	0.02	2.58	2.55	0.03	4.60	4.58	0.02	4.10	3.96	0.14	–	–	–

	H1a	H1b	H2a/b	H3a/b	H6	H9	H11	H11a	H12a	H13	H14
SJG-136	2.55	3.21	5.84	4.02/4.06	7.05	6.53	5.64	3.92	4.24	2.28	3.83

The imine (or iminium) form reacts as an electrophile with the exocyclic NH_2 group of a guanine base and, therefore, only one reaction site is available to this drug on each strand of DNA. Connectivities between SJG-136 and the duplex are listed in Table 2. These, along with the large chemical shift changes throughout the central bases of the adduct when compared with the duplex (Table 1), confirm the presence of the drug in the minor groove. Similar shift changes were previously reported for the DSB-120 adduct with an identical duplex.[24] In light of this evidence, the covalent linkage site is identified as G4, supported by large changes in the chemical shift of the opposite base (C7) as well as of I8.

Stereochemical Configuration and Orientation of the Ligand. It is possible, in principle, for the covalent linkage site C11 to have an *R* or *S* stereochemical configuration in PBD−DNA adducts. Previous studies have shown that, for the tomaymycin d(ATGCAT)$_2$ adduct, the PBD-11-*R* and PBD-11-*S* stereoisomers exist in approximately equal amounts.[37] However,

dx.doi.org/10.1021/bi102017e |*Biochemistry* 2011, 50, 4720–4732

Table 2. NOE Connectivities Observed between Protons on the Covalently Bound SJG-136 and the 5′-d(CICGATCICG)$_2$ Duplex[a]

	SJG-136 Protons (PBD residue bound to G4)										
	H1a	H1b	H2a/b	H3a/b	H6	H9	H11	H11a	H12a/b	H13a/b	H14
G4 H4′			W								
G4 H1′							M				
A5 H2						S			M	W	
A5 H1′				W			M				
A5 H4′			M	W			W				
A5 H3′				M							
T6 H4′					M				W		W
T6 H5′					W						
T6 H5″					W						
T6 H1′						M			M	M	
C7 H1′		W				W		W	M	M	W
C7 H4′						W			W	S	W
I8 H3′	M	M									
I8 H2	M	M	W				W	M			
I8 H4′				W	W			W			
I8 H1′				W				M			
C9 H4′			M	W				W			
C9 H1′				W							

[a] Abbreviations: S, strong; M, medium; W, weak.

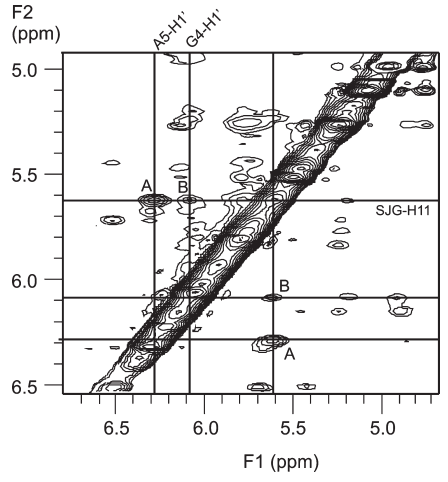

Figure 3. Two-dimensional 600 MHz NOESY spectrum of the 5′-d(CICGATCICG)$_2$−SJG-136 adduct with a 200 ms mixing time. NOE connectivities between SJG H11 and DNA H1′ are shown, confirming the *S* configuration at C11.

molecular mechanics calculations predict that the lower-energy conformation is 11-*S*,[38−40] and other studies have shown the *S* stereoisomer to be predominant for this class of drugs.[41,42] The proton attached at the PBD C11 covalent linkage site has proven to be a useful diagnostic probe for determination of the configuration at this site. It has been stated that, in an adduct with the *S* configuration at PBD C11, H11 of PBD will be directed toward the 3′-side of the covalently modified guanine, whereas, for an *R*-isomer, the situation is reversed, with H11 of PBD closer to the 5′-side.[24] In the case of the 5′-d(CICGATCICG)$_2$−SJG-136 adduct, a strong NOE between SJG H11 and A5 H1′ (Figure 3) confirms that the *S* isomer is present. This is supported by the absence of any cross-peak between SJG H11 and the cytosine to the 5′-side of G4 (C3). Analysis of DQF-COSY data gave a coupling constant of 11.0 Hz between the protons of C11 and C11a; this is only possible with an *S* configuration at C11. Predicted dihedral angles between bonds to protons at C11 and C11a for the *S* and *R* configurations have been previously reported to be 159° and 27°, respectively,[35] and the observed ^3J coupling confirms the *S* configuration at C11 within the SJG-136 duplex adduct.

A comparison of the 5′-d(CICGATCICG)$_2$−DSB-120 adduct[24] with the 5′-d(CICGATCICG)$_2$−SJG-136 adduct shows very similar two-dimensional NOESY spectra. However, some marked differences were observed. Although the chemical shift values for the two adducts were generally similar, there was a marked upfield shift in many of the signals of the DNA C9 base protons in the SJG-136 adduct, when compared with the DSB-120 adduct. This, along with changes in the relative shifts of the protons of DNA C1 and DNA I8, can be attributed to the anisotropic shielding effect of the C-ring methylidene group.

Chemical shifts of H2′ and H2″ resonances are usually seen between δ 1.5 and 3.0. The H1′−H2′ NOE is invariably more intense than the H1′−H2″ NOE as a result of the greater interproton distance in the latter case, and typically, the H2′ protons resonate upfield of the H2″ protons within the same nucleotide sequence.[24] For the I8 nucleotide in the SJG-136 adduct, however, there is a reversal of the general pattern and the H1′−H2″ cross-peak is found upfield of the H1′−H2′ cross-peak. This feature was also noted in the study of the DSB-120 adduct and is indicative of a conformational change within the internal nucleotide. It suggests that, as with DSB-120, SJG-136 induces an additional perturbation in the structure of the C7 nucleotide facing the covalently modified G4 in the minor groove.

Chemical Shift Changes in the 5′-d(CICGATCICG)$_2$−SJG-136 Adduct Compared to Duplex DNA. Chemical shifts for oligonucleotide proton resonance signals of the SJG-136 adduct relative to the duplex are listed in Table 1. There are upfield chemical shifts of 0.39 and 0.26 ppm for C7 H6 and C7 H5, respectively, which mirror shift changes seen when the same duplex sequence reacted with DSB-120. In addition, large chemical shift changes can be seen for C7 H2′/H2″ and C7 H3′ signals. These chemical shift changes suggest an increase in the level of stacking at the T6-C7 step. However, studies of the DSB-120 adduct revealed probable destacking of the I2-C3 step, deduced from downfield shifts for C3 H6 and C3 H5. These

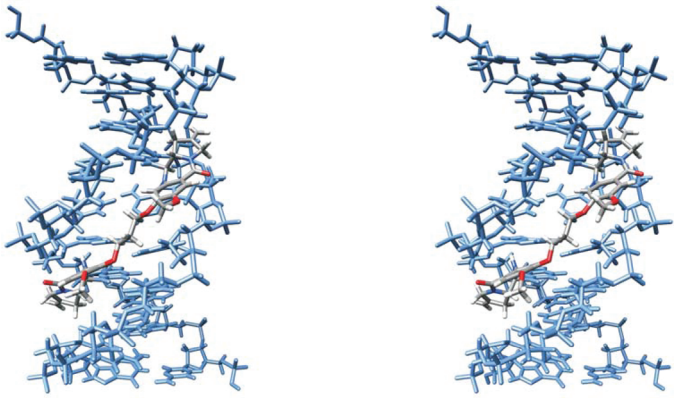

Figure 4. Stereoview of the 5′-d(CICGATCICG)$_2$−SJG-136 intrastrand adduct. DNA strands are colored blue, and SJG-136 is shown in atom colors. Watson−Crick base pairing has been maintained, and there is minimal distortion to the β-helical structure of the DNA backbone. Models were produced in the SYBYL modeling suite and images produced using UCSF Chimera.[44]

shifts are absent from the spectrum of the SJG-136 adduct, suggesting that the aforementioned destacking does not occur in this case. The I8 H2 resonance of the SJG-136 adduct undergoes a 0.34 ppm upfield shift. Similar observations were noted in the relative chemical shifts of I8 H2 when the duplex sequence reacted with tomaymycin.[16] A large upfield shift of the I8 H2 signal relative to the duplex was attributed to the shielding effect of the ethylidene functionality of the drug in this case. This shift is not seen in the DSB-120 adduct because of the absence of the ethylidene group, and in the case of SJG-136, it would appear that the introduction of the ethylene functionality produces an effect similar to that of tomaymycin. The 0.34 ppm downfield shift of the A5 H5 resonance has also been seen in both the DSB-120 and tomaymycin adducts and can be attributed to deshielding effects of the aromatic ring of the covalently attached drug. Other chemical shift changes within the adduct relative to the duplex, as seen with DSB-120, occur mainly for protons in the proximity of the attached drug, and most can be attributed to drug shielding and deshielding effects.

The previous studies of DSB-120[24] and tomaymycin[16] highlighted a dramatic difference between the magnitude of the chemical shift changes of T6 H4′ in the adducts. This proton is shielded by the drug aromatic rings in both cases, but the resulting upfield shift was dramatically attenuated in the case of DSB-120. It is suggested by the authors[24] that the structure of the interstrand cross-linking via tethered DNA reactive units in this case causes the DSB aromatic rings to be partially averted from the wall of the groove, greatly reducing the level of shielding experienced. In the case of SJG-136, an only 0.22 ppm upfield shift is observed, compared with 1.65 ppm in the case of DSB-120. This suggests that, in this case, the aromatic rings of the drug are averted still further, causing the shielding to be much weaker relative to that felt by DSB-120.

Intermolecular Drug−DNA Contacts. The proton resonances for SJG-136 were identified and assigned via analysis of the NOESY and COSY spectra. Contacts have been found between SJG-136 protons and G4, A5, T6, C7, I8, and C9 bases and are listed in Table 2. The presence of this network of NOE contacts from SJG-136 to specific DNA protons locates the drug indisputably in the minor groove. As seen in studies of the DSB-120 adduct, SJG H11 shows a strong cross-peak to A5 H1′ and a moderate cross-peak to G4 H1′. In the case of DSB-120, further evidence of the averted aromatic ring discussed above was found on the basis of the intensity of the cross-peak between SJG H11 and A5 H4′. Unfortunately, in this study, the cross-peak in question is situated under the large COSY peak arising from the scalar coupling of SJG H11 to SJG H11a, so no such conclusions can be drawn. However, the methylene protons of the linker (SJG H12a, H12b, H13a, and H13b) all exhibit expected NOESY connectivities that locate them definitively in the minor groove. As with DSB-120, the characteristic signal between SJG H13a/b and C7 H4′, although overlaid, can be located as a strong cross-peak, while SJG H12a and SJG H12b show connectivities to A5 H2 and T6 H1′. Interestingly, evidence based on connectivities from SJG H1a and SJG H1b of SJG-136 to I8 H2 and I8 H1′ suggests that this drug is located more deeply in the minor groove than DSB-120. In the study of the latter drug, DSB H1a and DSB H1b both show very weak NOESY cross-peaks to I8 H2 and I8 H1′, and from these diminished through-space connectivities, it was deduced that DSB-120 was immersed rather shallowly in the minor groove. In the SJG-136 adduct of our study, SJG H1a and SJG H1b show relatively intense cross-peaks to I8 H2. Unfortunately, as with A5 H4′, the SJG H1a− and SJG H1b−I8 H1′ resonance is too overlaid to be conclusive. However, the deeper location of SJG-136 in the minor groove is further supported by the apparent absence of cross-peaks between SJG H1a/b and A5 H1′ or C7 H4′. Three of these peak areas are overlaid, but there is a clear absence of any connectivity between SJG H1a and C7 H4′. This suggests that the SJG-136 adduct bears a greater resemblance to the tomaymycin adduct, in this respect, than to DSB-120, where a bowing of the ends of the drug away from the floor of the minor groove resulted in weak NOEs being observed between the protons discussed above.

Refined Molecular Model of the 5′-d(CICGATCICG)$_2$−SJG-136 Adduct. The 5′-d(CICGATCICG)$_2$−SJG-136 interstrand adduct was modeled using the SYBYL-X 1.0 modeling package. Figure 4 shows the in aquo computer model of the interstrand adduct. SJG-136 is depicted in gray and atom colors, with the two DNA strands colored blue. Watson−Crick base pairing has been maintained throughout the duplex adduct.

5′-d(CTCATCAC)·(GTGATGAG)−SJG-136 Intrastrand Adduct. *Design and Synthesis of the Duplex.* The 5′-d(CTCATCAC)·(GTGATGAG) duplex was designed to afford no reaction sites on the "C" strand, while providing two available sites on the "G" strand for the investigation of the possibility of formation of an

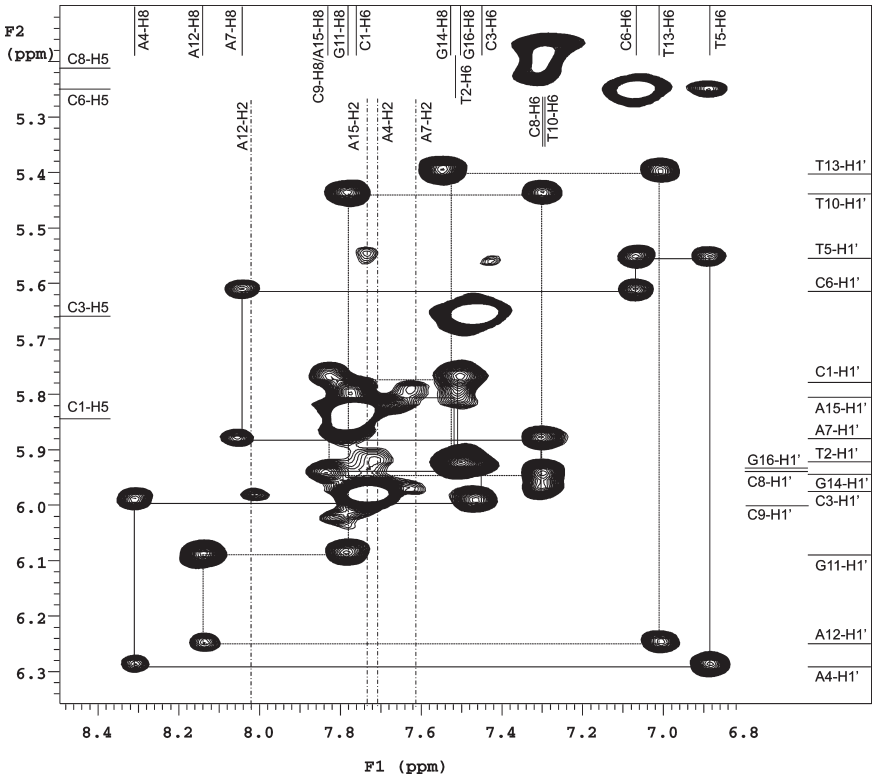

Figure 5. Two-dimensional phase-sensitive NOESY spectrum (200 ms mixing time) expanded contour plot of the SJG-136 intrastrand cross-linked duplex adduct in buffered D_2O solution (pH 6.75) at 300 K, displaying connectivities from aromatic PuH8/PyH6 to deoxyribose H1′ and deoxyribose H1′ of the 5′-neighbor.

Table 3. Chemical Shift Assignments for SJG-136 Protons in the 5′-d(CTCATCAC)·(GTG^{14}ATG^{11}AG)−SJG-136 Adduct

	H8/H6			H1′			H2′			H2″			H3′			H4′			CH_3/H2/H5		
	duplex	adduct		duplex	adduct		duplex	adduct		duplex	adduct		duplex	adduct		duplex	adduct		duplex	adduct	
C1	7.70	7.76	0.06	5.67	5.80	0.13	2.04	2.08	0.02	2.38	2.44	0.06	4.46	4.55	0.09	3.90	3.98	0.08	5.76	5.84	0.08
T2	7.48	7.52	0.04	5.96	5.93	0.03	2.04	2.15	0.11	2.40	2.44	0.04	4.70	4.79	0.09	4.05	4.13	0.17	1.50	1.58	0.08
C3	7.42	7.45	0.05	5.34	5.99	0.65	1.98	2.12	0.14	2.26	2.55	0.29	4.40	4.82	0.42	3.96	4.18	0.22	5.56	5.65	0.09
A4	8.18	8.32	0.14	6.05	6.29	0.24	2.47	2.75	0.28	2.74	2.60	0.14	4.83	4.89	0.06	3.96	3.89	0.07	7.45	7.73	0.28
T5	7.00	6.89	0.11	5.66	5.55	0.11	1.84	2.18	0.34	2.24	1.76	0.48	4.64	4.51	0.13	3.96	3.56	0.40	1.24	1.15	0.09
C6	7.35	7.07	0.28	5.37	5.61	0.24	1.86	2.12	0.26	2.18	1.64	0.54	4.64	4.71[a]	0.07	3.90	3.94	0.04	5.46	5.25	0.21
A7	8.10	8.04	0.06	6.03	5.88	0.13	2.46	2.53	0.07	2.66	2.42	0.24	4.83	4.78	0.05	3.96	3.62	0.34	7.67	7.61	0.06
C8	7.19	7.30	0.11	5.86	5.97	0.11	1.90	1.97	0.07	2.64	2.02	0.62	4.60	4.71[a]	0.11	4.27	4.04	0.23	5.20	5.21	0.01
G9	7.77	7.83	0.07	5.80	5.94	0.14	2.05	2.47	0.42	2.60	2.72	0.12	4.77	4.71[a]	0.06	3.90	4.13	0.23	–	–	–
T10	7.19	7.30	0.11	5.64	5.44	0.20	1.98	2.42	0.44	2.32	2.22	0.10	4.70	4.82	0.12	4.03	4.13	0.10	1.20	1.39	0.19
G11	7.73	7.78	0.05	5.48	6.08	0.60	2.51	2.84	0.33	2.62	2.60	0.02	4.83	4.97	0.14	4.16	4.35	0.19	–	–	–
A12	8.04	8.14	0.10	6.01	6.24	0.23	2.41	2.55	0.14	2.70	2.44	0.26	4.76	4.86	0.10	4.26	3.86	0.40	7.60	8.02	0.42
T13	6.86	7.01	0.15	5.46	5.40	0.06	1.68	2.15	0.47	2.04	2.10	0.06	4.83	4.60	0.23	3.89	3.45	0.44	1.19	1.26	0.07
G14	7.66	7.52	0.14	5.19	5.94	0.85	2.32	2.45	0.13	2.44	2.57	0.13	4.62	4.55	0.07	4.10	4.05	0.05	–	–	–
A15	7.92	7.83	0.09	7.60	7.71	0.11	5.92	5.77	0.15	2.44	2.44	0.00	2.68	2.55	0.13	4.76	4.87	0.11	4.23	4.05	0.18
G16	7.44	7.51	0.07	–	–	–	5.78	5.92	0.13	2.16	2.08	0.08	2.38	2.55	0.17	4.82	4.47	0.37	*a*	3.98	–

	H1a	H1b	H2a	H2b	H3a	H3b	H6	H9	H11	H11a	H12a	H12b	H13b	H13a	H14
SJG-136 (linked to G14)	2.95	2.58	5.32	5.17	4.32	4.11	6.95	5.97	4.52	4.74	4.25	3.76	2.30	2.07	3.80
	H1a′	H1b′	H2a′	H2b′	H3a′	H3b′	H6′	H9′	H11′	H11a′	H12a′	H12b′	H14′		
SJG-136 (linked to G11)	3.22	2.64	5.24	5.22	4.09	4.14	7.06	6.58	5.76	3.91	4.20	4.30	3.78		

[a] We assume the signal was lost with water suppression.

dx.doi.org/10.1021/bi102017e |*Biochemistry* 2011, 50, 4720–4732

Table 4. NOE Connectivities Observed between Protons on the Covalently Bound SJG-136 and the 5′-d(CTCATCAC)·(GTGATGAG) Duplex[a]

	SJG-136 Protons (PBD residue covalently bound to G11)													
DNA proton	H1a′	H1b′	H2a′	H2b′	H3a′	H3b′	H6′	H9′	H11′	H11a′	H12a′	H12b′	H13a/b	H14′
A4 H2												W		
C6 H1′								M		S	S	M		
C8 H1′		M	W											
A7 H2	S	M	W	W					W	M				
A7 H1′	M	M			W	W				S				
A7 H3′														M
A7 H4′							M		W					S
G11 H1′			S	S										
G11 H4′			M	M										
A12 H2								S			M	M	M	
A12 H1′								W						
A12 H4′	M	M	W	M										
T13 H1′								M			M	M		
T13 H4′							W	W					W	
G14 H4′													S	

	SJG-136 Protons (PBD residue covalently bound to G14)													
DNA proton	H1a	H1b	H2a	H2b	H3a	H3b	H6	H9	H11	H11a	H12a	H12b	H13a/b	H14
C3 H1′			W											
A4 H1′						M		W	M					
A4 H2								S			M	M		
A4 H4′			M	M										
T5 H1′								M			M	M		
T5 H4′							S							
A12 H2											W	M	M	
T13 H1′								W			M	M		
T13 H4′													W	
A15 H1′	S	S			M									
A15 H2	W	M												
A15 H4′										M				
G16 H4′	W	W												

[a] Abbreviations: S, strong; M, medium; W, weak.

intrastrand cross-link. SJG-136 is known to react through the exocyclic NH_2 group of a guanine base. This means that the only possible reaction sites for the drug within the 5′-d(CTCATCAC)·(GTG*ATG*AG) duplex are bases G11 and G14, as shown in Figure 1. SJG-136 has been previously shown to cover a 3 bp region; hence, DNA bases G9 and G14 are situated too far apart for cross-linking.[23]

Confirmation of the Formation of Cross-Links with Two Alkylation Sites. Assignment of the proton NMR signals of the 5′-d(CTCATCAC)·(GTGATGAG)−SJG-136 adduct used standard COSY and NOESY NMR techniques. An expansion of the H8/H6−H1′ region of the duplex and adduct NOESY spectra can be seen in Figure 5. After reaction with SJG-136, there are no duplex resonances remaining in the adduct spectrum, confirming that the reaction has proceeded to completion.

Four COSY peaks can be identified in the aromatic region, confirming the presence of four discrete cytosine residues and confirming that a single adduct formed. The presence of two aromatic H1′ "walks" and relative NOE intensities in this region confirms that the DNA duplex has retained its B-form character. In addition, SJG-136 signals that confirm two reaction sites can be identified, indicating that the drug has reacted at both ends forming a non-self-complementary bis-adduct. Complete chemical shift assignments for the nucleotide and drug protons in the duplex and the adduct are listed in Table 3.

Identification of the Covalent Linkage Site. As with the 5′-d(CICGATCICG)$_2$−SJG-136 adduct, large chemical shift changes at G14 H1′ and G11 H1′ (0.85 and 0.60 ppm, respectively), as well as in their paired cytosines, confirm the sites of covalent modification. Large chemical shift changes are also seen for the central protons A4 H1′ and T5 H1′ (C strand) and T13 H1′ and A12 H1′ (G strand). In addition, relatively large changes (>0.20 ppm) are seen for several of the G strand H2″ protons (G9 H2″, T10 H2″, and T13 H2″). This is suggestive of a stronger association of the drug with the modified strand and is not unexpected. Connectivities between SJG-136 and the duplex were numerous and are listed in Table 4. These connectivities, in conjunction once again with large chemical shift changes throughout the central bases of the duplex adduct, place the drug unequivocally within the minor groove.

dx.doi.org/10.1021/bi102017e |*Biochemistry* 2011, 50, 4720–4732

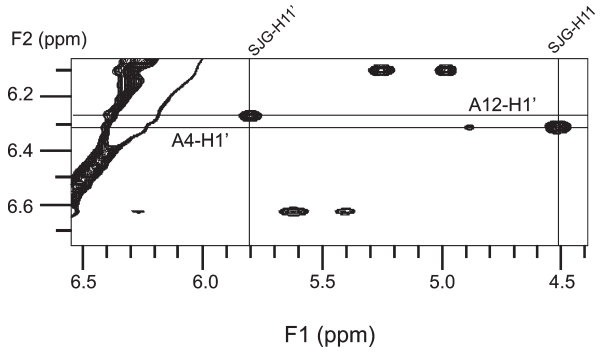

Figure 6. NOESY spectrum (600 MHz) of the 5′-d(CTCATCAC)·(GTGATGAG)−SJG-136 adduct, with a 200 ms mixing time. Expansion showing NOE connectivities between SJG H11 and A12 H1′ and between SJG H11′ and A4 H1′ as confirmation of the *S* configuration at the SJG C11 and SJG C11′ centers.

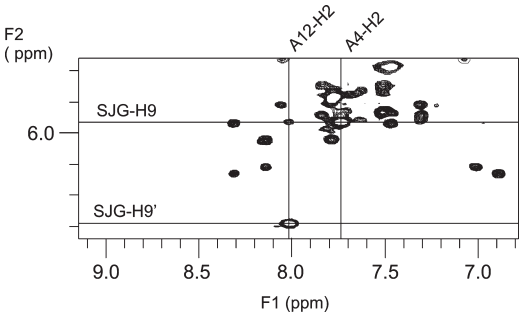

Figure 7. Two-dimensional 600 MHz NOESY spectrum of the 5′-d(CTCATCAC)·(GTGATGAG)−SJG-136 adduct, with a 200 ms mixing time. Expansion showing NOE connectivities between SJG and H9 and H9′ and A H2 protons.

Stereochemical Configuration of Alkylation Sites. The proton attached at the C11 covalent linkage site is a useful diagnostic probe for the determination of *R* or *S* configuration.[24] In an adduct with *S* configuration, SJG H11 will be directed toward the 3′-side of the covalently modified guanine; conversely, in an *R* isomer, a reversed situation would be observed with SJG H11 closer in space to the 5′-side. In this study, the 5′-end (G11) of the duplex shows a strong NOE between SJG H11 and A12 H1′ (Figure 6). This confirms that the configuration at SJG C11 is *S* at this end of the molecule. This is not unexpected, as both the SJG-136 intrastrand adducts and the 5′-d(CICGATCICG)$_2$−DSB-120 adduct[24] had the *S* configuration at this site. At the 3′-end of the duplex, the PBD subunit is a mirror image of that at the 5′-end. A C11 chiral center with the *S* configuration will, therefore, direct its proton toward the 3′-neighbor of G14's base-paired cytosine on the opposite strand (A4). The *R* configuration would result in an enhanced connectivity with G14's 3′-neighbor, A15. When the two-dimensional NOESY spectrum for the 5′-d(CTCATCAC)·(GTGATGAG)−SJG-136 adduct was examined, there was no connectivity between SJG H11 and A15 H1′; however, a large NOE is seen between SJG H11 and A4 H1′ (Figure 6). This indicates that the 3′-end of the drug adduct also has the *S* configuration, in accordance with previous studies on interstrand adducts.[24,43] In addition to NOE evidence, analysis of DQF-COSY data gave coupling constants between the C11 and C11a protons of 11.1 Hz (G11) and 11.0 Hz (G14); these results, as for the interstrand adduct, confirm the *S* configuration for C11 at both alkylation sites.

Relative Chemical Shifts of DNA H2′ and H2″. In general, the H2′ protons resonate upfield of the H2″ protons within the same nucleotide sequence.[24] Upon assignment of the 5′-d(CICGATCICG)$_2$−SJG-136 spectrum, a reversal in the general pattern for H1′−H2′/H2″ resonances was noted for the I8 nucleotide, with the more intense H1′−H2′ NOE found downfield of the H1′−H2″ NOE. This was attributed to a conformational change within the internal nucleotide, with an additional perturbation of the structure of the nucleotide facing the covalently modified guanine. In the case of the 5′-d(CTCATCAC)·(GTGATGAG)−SJG-136 adduct, a similar reversal of the general pattern is seen in many of the nucleotides in the vicinity of the drug. This is, perhaps, to be expected with the accommodation of SJG-136 in the minor groove as an intrastrand adduct, and perturbation of the surrounding nucleotides provides additional evidence that supports this proposal.

Location of the SJG-136 Residue within the Duplex Adduct. Chemical shifts for the oligonucleotide proton resonance signals of the SJG-136 adduct relative to the duplex are listed in Table 3. Numerous large resonance shifts can be seen, which would be expected upon accommodation of the ligand in the minor groove in this way. The two central adenine H2 resonances (A4 H2 and A12 H2) both experience large downfield shifts of 0.28 and 0.42 ppm, respectively, providing further evidence of some central perturbation as a result of formation of an intrastrand adduct. Upon examination of the H1′ and H2′ chemical shift data, it can be seen that a majority of large shift changes from duplex to adduct are found in nucleotides situated on the covalently modified DNA strand. This suggests that the drug is associating more closely with the modified strand and, as such, supports the identification of the intrastrand adduct.

The proton resonances for two PBD residues in SGJ-136 were identified and assigned using analysis of the COSY and NOESY correlations. Numerous NOE correlations were then established between the SJG-136 protons and the protons on the C3, A4, T5, C6, and A7 nucleotides on the noncovalently modified strand and the G11, A12, T13, G14, and A15 nucleotides on the covalently modified strand. These are listed in Table 4.

Absolute confirmation of the orientation of the SJG-136 molecule was achieved with a strong NOE contact between SJG H9 and the respective A H2 protons of the central adenine nucleotides (A12 H2 and A4 H2) of the DNA duplex. These appear in the H6/H8−H1′ region of the spectrum (Figure 7). These assignments are confirmed by the presence of further NOE contacts between the SJG H9 and H9′ protons at the respective ends of the drug and the surrounding DNA protons. The SJG H1a/b and H1a/b′ proton signals were assigned on the basis of their respective proximity to the nearby adenine H2 (A7 H2 and A15 H2), as well as through NOE cross-peaks to other drug resonances. Using a preliminary unrefined model, it can be seen that SJG H1a will be closer in space to the A H2 than SJG H1b, the two were therefore assigned using the size of the resulting NOE cross-peak. In addition, SJG H1a gives rise to more intense cross-peaks than SJG H1b, H11, and H2a/b, reflecting the fact that SJG H1a is closer in space to these protons than SJG H1b.

The SJG H2a/b protons were similarly assigned on the basis of their proximities to surrounding protons. Unfortunately, in this case, connectivities to the DNA backbone were too overlaid to be of use, so SJG H2a/H2a′ and SJG H2b/H2b′ were distinguished by their NOE contacts with other drug resonances. When models of the 5′-d(CTCATCAC)·(GTGATGAG)−SJG-136 adduct

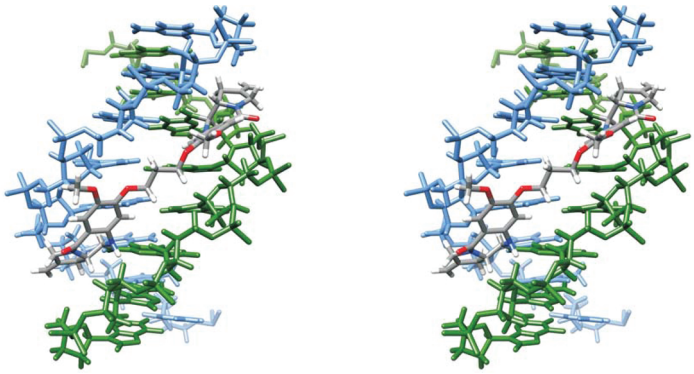

Figure 8. Stereoview of the 5′-d(CTCATCAC)·(GTGATGAG)−SJG-136 intrastrand adduct. DNA strands are colored green (modified) and blue, and SJG-136 is shown in atom colors. Watson−Crick base pairing has been maintained, and there is minimal distortion to the β-helical structure of the DNA backbone. Models were produced in the SYBYL modeling suite and images using UCSF Chimera.[44]

are examined, it can be seen that SJG H2a/H2a′ is closer in space to SJG H1/H1′, whereas SJG H2b/H2b′ is closer to SJG H3/H3′. When these NOE connectivities are examined, it is observed that the intensities of the cross-peak vary significantly, and SJG H2a/b/H2a/b′ were assigned on this basis. This was supported for SJG H2a/b by the NOE cross-peaks to SJG H11a, in which SJG H2a displayed a slightly more intense resonance.

The SJG-H3a/b protons were distinguished as a result of small differences in spatial proximity to SJG H6 and H2a/b. When distances are measured from the preliminary unrefined molecular models, SJG H3a is slightly closer to SJG H2 protons than is SJG H3b. In addition, SJG H3b is marginally closer in space to the SJG H6 proton (∼0.5 Å based on preliminary unrefined models). When the two-dimensional NOESY NMR spectrum is examined, SJG H3a shows a more intense cross-peak to SJG H2a/b than does SJG H3b. Upon examination of the SJG H6 connectivities, it is observed that a weak NOE to SJG H3b exists, while there is no connectivity with SJG H3a. On this basis, a distinction was made between SJG H3a and SJG H3b. At the G 5′-end of the molecule, the SJG H3a/b′ protons were too overlaid to allow distinction to be made between them; consequently, they are reported as SJG H3a/b′. The SJG H12a/b and H12a/b′ signals were difficult to distinguish because of their resonance in the overcrowded H4′ region of the spectrum. However, they are tentatively assigned on the basis of connectivities to SJG H9′ and adenine protons, A12 H2 and A4 H2. The SJG H12a′ proton shows a more intense cross-peak to SJG H9′ than does SJG H12b′, so a distinction can be made between the two. At the 3′-end of the molecule, the NOE connectivities from SJG H12a/b to A4 H2 and A12 H2 show significant differences, with a more intense cross-peak seen due to connectivity with SJG H12a in both cases. Finally, the SJG H13a/b protons were distinguished because of their NOE connectivity with SJG H9′. The distance between SJG H13b and SJG H9′ is greater than for SJG H13a, and upon examination of the spectrum, it can be seen that the cross-peak between SJG H9′ and SJG H13a is more intense.

An interesting feature of the intrastrand two-dimensional NOESY spectrum is the unusually low chemical shift of T13 H4′ and T5 H4′. These nucleotides are situated at the center of the duplex, between the two sites of covalent modification. The enhanced shielding of the 4′-protons in these bases is probably due to the proximity of the aromatic PDB rings and indicates some distortion around the SJG C11 center.

Refined Molecular Model of the 5′-d(CTCATCAC)·(GTGATGAG)−SJG-136 Adduct. The 5′-d(CTCATCAC)·(GTGATGAG)−SJG-136 intrastrand adduct was modeled using the SYBYL-X 1.0 modeling package. Figure 8 shows the in aquo computer model of the intrastrand adduct. SJG-136 is depicted in gray and atom colors, with the two DNA strands colored green and blue. As with the interstrand adduct, it is clear that Watson−Crick base pairing has been maintained. This is in agreement with the two-dimensional NMR spectra, which is concordant with maintenance of the β-helical structure of the DNA backbone.

DISCUSSION

In summary, an interstrand cross-linked DNA adduct with 5′-d(CICGATCICG)$_2$ has been synthesized, characterized, and modeled. This adduct is similar to the previously reported DSB-120 duplex adduct with the same DNA sequence.[24] However, this adduct also has some of the characteristics of the bistomaymycin adduct previously reported,[16] with the ligand being located more deeply in the minor groove than predicted and the two PBD residues tilted such that the unsaturated methylenes are raised up from the base of the minor groove.

A second intrastrand adduct with the 5′-d(CTCATCAC)·(GTGATGAG) duplex has also been prepared, fully assigned, and modeled. Covalent linkage sites have been confirmed to be the exocyclic NH$_2$ groups of DNA G11 and DNA G14, making this the first positive identification of an intrastrand cross-linked DNA−PBD adduct. The stereochemical configurations at the SJG C11 alkylation sites have been confirmed as *S* at both ends of the duplex, in agreement with molecular mechanics energy calculations that predict that the *S* configuration at C11 of SJG is energetically favored.[38−40]

Relative chemical shifts of DNA H2′ and H2″ have been found to show a reversal in the usual pattern for duplex DNA, with the more intense DNA H1′−DNA H2′ resonance found downfield of the DNA H1′−DNA H2″ resonance. This has been noted in previous studies of DNA−PBD adducts, both within this study and in studies of the DSB-120 adduct,[24] and is indicative of a conformational change within the internal nucleotide. This was not unexpected upon accommodation of an intrastrand cross-linkage. In both the inter- and intrastrand duplex adducts, intermolecular drug−DNA contacts confirm the presence of the ligand located in the minor groove and following the right-handed contour of the β-helical DNA helix. In addition, NOE

connectivities in the intrastrand adduct suggest that the SJG-136 molecule associates more closely with the covalently modified strand.

The results of this study in combination with the results of the HPLC and MS studies[23] are important in establishing the mechanism of action for these compounds, and this is particularly important to those involved in the preclinical and clinical development of these compounds. Before this study, it was believed that the antitumor activity of these compounds was exclusively due to the formation of interstrand cross-links at purine-GATC-pyrimidine sequences, and both preclinical and clinical evaluation has focused on this activity.[44,45] Cross-links at purine-GATC-pyrimidine sites have been measured in in vitro cell-based experiments and in peripheral blood lymphocytes (PBLs) during the phase I clinical trials using the COMET[46,47] and γH2AX-foci[48] assays. Further studies will now be required to establish the significance of these adducts and determine if activity is purely down to interstrand cross-linking or a combination of interstrand cross-linking, intrastrand cross-linking, and monoalkylation. The inter- and intrastrand cross-links produced by SJG-136 will be repaired in vivo via different mechanisms, and the significance of this should also be established, as it is possible this dual functionality will limit the ability of cancer cells to develop resistance to these compounds.

This study also shows how the binding of these compounds is significantly altered by the substituents and saturation of the pyrrolo ring, an observation previously restricted to naturally occurring and synthetic monoalkylating PBDs. This opens up new avenues for the design of third-generation PBD dimers incorporating additional features from the more potent PBD monomers and also targeting specific types of cross-links to establish the relative importance of each type of ligand interaction.

■ ASSOCIATED CONTENT

Supporting Information. Two-dimensional NOESY spectrum of the 5′-d(CTCATCAC)·(GTGATGAG)−SJG-136 adduct with a 200 ms mixing time, with expansions showing NOE connectivities between SJG H9 and H9′ and DNA H1′. This material is available free of charge via the Internet at http://pubs.acs.org.

■ AUTHOR INFORMATION

Corresponding Author

*E-mail: a.s.thompson@bath.ac.uk. Telephone: 00 44 1225 386765. Fax: 00 44 1225 386114.

Funding Sources

This research was funded by the University of Bath through a studentship to S.R.H. We thank Ipsen for providing the SJG-136.

■ ACKNOWLEDGMENT

We thank Dr. Timothy J. Woodman (University of Bath) for his help gathering the NMR data and Professor Michael D. Threadgill (University of Bath) for proofreading the manuscript. Molecular graphics images were produced using UCSF Chimera[36] from the Resource for Biocomputing, Visualization, and Informatics at the University of California, San Francisco (supported by National Institutes of Health Grant P41 RR001081).

■ ABBREVIATIONS

PBD, pyrrolo[2,1-*c*][1,4]benzodiazepine; NMR, nuclear magnetic resonance; NOE, nuclear Overhauser effect; NOESY, two-dimensional NOE correlated spectroscopy; rMD, restrained molecular dynamics; rMM, restrained molecular mechanics; FID, free induction decay; DMF, dimethylformamide; EDTA, ethylenediaminetetraacetic acid; HPLC, high-performance liquid chromatography; MS, mass spectroscopy.

■ REFERENCES

(1) Thurston, D. E. (1993) Advances in the study of pyrrolo[2,1-c][1,4]benzodiazepine (PBD) antitumor antibiotics. In *Molecular aspects of anticancer drug-DNA interactions* (Neidle, S., and Waring, M. J., Eds.) pp 54−88, The Macmillan Press Ltd., London.

(2) Hurley, L. H., Reck, T., Thurston, D. E., Langley, D. R., Holden, K. G., Hertzberg, R. P., Hoover, J. R., Gallagher, G., Faucette, L. F., Mong, S. M., and Johnson, R. K. (1988) Pyrrolo(1,4)benzodiazepine antitumor antibiotics: Relationship of DNA alkylation and sequence specificity to the biological activity of natural and synthetic compounds. *Chem. Res. Toxicol. 1*, 258–268.

(3) Bose, D. S., Thompson, A. S., Ching, J., Hartley, J. A., Berardini, M. D., Jenkins, T. C., Neidle, S., Hurley, L. H., and Thurston, D. E. (1992) Rational design of a highly efficient irreversible DNA interstrand cross-linking agent based on the pyrrolobenzodiazepine ring system. *J. Am. Chem. Soc. 114*, 4939–4941.

(4) Bose, D. S., Thompson, A. S., Smellie, M., Berardini, M. D., Hartley, J. A., Jenkins, T. C., Neidle, S., and Thurston, D. E. (1992) Effect of linker length on DNA-binding affinity, cross-linking efficiency and cytotoxicity of C8-linked pyrrolobenzodiazepine dimers. *J. Chem. Soc., Chem. Commun. 14*, 1518–1520.

(5) Thurston, D. E., Bose, D. S., Thompson, A. S., Howard, P. W., Leoni, A., Croker, S. J., Jenkins, T. C., Neidle, S., Hartley, J. A., and Hurley, L. H. (1996) Synthesis of sequence selective C8-linked pyrrolo-[2,1-*c*][1,4]benzodiazepine DNA interstrand crosslinking agents. *J. Org. Chem. 61*, 8141–8147.

(6) Gregson, S. J., Howard, P. W., Hartley, J. A., Brooks, N. A., Adams, L. J., Jenkins, T. C., Kelland, L. R., and Thurston, D. E. (2001) Design synthesis and evaluation of a novel pyrrolobenzodiazepine DNA-interactive agent with highly efficient cross-linking ability and potent cytotoxicity. *J. Med. Chem. 44*, 737–738.

(7) Gregson, S. J., Howard, P. W., Gullick, D. R., Hamaguchi, A., Corcoran, K. E., Brooks, N. A., Hartley, J. A., Jenkins, T. C., Patel, S., Guille, M. J., and Thurston, D. E. (2004) Linker length modulates DNA cross-linking reactivity and potency for ether-linked C2-exo-unsaturated pyrrolo-[2,1-c][1,4]benzodiazepine (PBD) dimers. *J. Med. Chem. 47*, 1161–1174.

(8) Farmer, J. D., Rudnicki, S. M., and Suggs, J. W. (1988) Synthesis and DNA crosslinking ability of a dimeric anthramycin analog. *Tetrahedron Lett. 29*, 5105–5108.

(9) Smellie, M., Bose, D. S., Thompson, A. S., Jenkins, T. C., Hartley, J. A., and Thurston, D. E. (2003) Sequence selective recognition of duplex DNA through covalent interstrand crosslinking: Kinetic and molecular modelling studies with pyrrolobenzodiazepine (PBD) dimers. *Biochemistry 42*, 8232–8239.

(10) Hochhauser, D., Meyer, T., Spanswick, V. J., Wu, J., Clingen, P. H., Loadman, P., Cobb, M., Gumbrell, L., Begent, R. H., Hartley, J. A., and Jodrell, D. (2009) Phase 1 study of a sequence selective minor groove DNA binding agent (SJG-136) with pharmacokinetic and pharmacodynamic measurements in patients with advanced solid tumors. *Clin. Cancer Res. 15*, 2140–2147.

(11) Puzanov, I., Lee, W., Berlin, J. D., Calcutt, M. W., Hachey, D. L., Vermeulen, W. L., Spanswick, V. J., Hartley, J. A., Chen, A. P., and Rothenberg, M. L. (2008) Final results of phase I and pharmacokinetic trial of SJG-136 administered on a daily × 3 schedule. *J. Clin. Oncol. 26*, Abstract 2504.

(12) Janjigian, Y. Y., Lee, W., Kris, M. G., Miller, V. A., Krug, L. M., Azzoli, C. G., Senturk, E., Calcutt, M. W., and Rizvi, N. A. (2010) A phase

I trial of SJG-136 (NSC694501) in advanced solid tumors. *Cancer Chemother. Pharmacol. 65*, 833–838.

(13) Hartley, J. A., Hamaguchi, A., Coffils, M., Martin, C. R. H., Suggitt, M., Chen, Z., Gregson, S. J., Masterson, L. A., Tiberghien, A. C., Hartley, J. M., Pepper, C., Lin, T. T., Fegan, C., Thurston, D. E., and Howard, P. W. (2010) SG2285, a novel C2-aryl-substituted pyrrolobenzodiazepine dimer prodrug that cross-links DNA and exerts highly potent antitumor activity. *Cancer Res. 70*, 6849–6858.

(14) Boyd, F. L., Cheatham, S. F., Remers, W., Hill, G. C., and Hurley, L. H. (1990) Characterization of the structure of the anthramycin d(ATGCAT)$_2$ adduct by NMR and molecular modeling studies, determination of the stereochemistry of the covalent linkage site, orientation in the minor groove of DNA, and effect on local DNA structure. *J. Am. Chem. Soc. 112*, 3279–3289.

(15) Krugh, T. R., Graves, D. E., and Stone, M. P. (1989) 2-Dimensional NMR studies on the anthramycin-d(ATGCAT)$_2$ adduct. *Biochemistry 28*, 9988–9994.

(16) Boyd, F. L., Stewart, D., Remers, W. A., Barkley, M. D., and Hurley, L. H. (1990) Characterization of a unique tomaymycin d-(CICGAATTCICG)$_2$ adduct containing two drug molecules per duplex by NMR, fluorescence, and molecular modeling studies. *Biochemistry 29*, 2387–2403.

(17) Kopka, M. L., Goodsell, D. S., Baikalov, I., Grzeskowiak, K., Cascio, D., and Dickerson, R. E. (1994) Crystal structure of a covalent DNA drug adduct: Anthramycin bound to CCAACGTTGG and a molecular explanation of specificity. *Biochemistry 33*, 13593–13610.

(18) Rao, S. N., and Remers, W. A. (1990) All atom molecular mechanics simulations on covalent complexes of anthramycin and neothramycin with deoxydecanucleotides. *J. Med. Chem. 33*, 1701–1707.

(19) Remers, W. A., Mabilia, M., and Hopfinger, A. J. (1986) Conformations of complexes between pyrrolo[1,4]benzodiazepines and DNA segments. *J. Med. Chem. 29*, 2492–2503.

(20) Jones, G. B., Davey, C. L., Jenkins, T. C., Kamal, A., Kneale, G. G., Neidle, S., Webster, G. D., and Thurston, D. E. (1990) The noncovalent interaction of pyrrolo[2,1-*c*][1,4]benzodiazepine-5,11-diones with DNA. *Anti-Cancer Drug Des. 5*, 249–264.

(21) Hertzberg, R. P., Hecht, S. M., Reynolds, V. L., Molineux, I. J., and Hurley, L. H. (1986) DNA-sequence specificity of the pyrrolo-[1,4]benzodiazepine antitumor antibiotic: Methidiumpropyl-EDTA-iron(II) footprinting analysis of DNA-binding sites for anthramycin and related drugs. *Biochemistry 25*, 1249–1258.

(22) Puvvada, M. S., Forrow, S. A., Hartley, J. A., Stephenson, P., Gibson, I., Jenkins, T. C., and Thurston, D. E. (1997) Inhibition of bacteriophage T7 RNA polymerase *in vitro* transcription by DNA-binding pyrrolo[2,1-*c*][1,4]benzodiazepines. *Biochemistry 36*, 2478–2484.

(23) Rahman, K. M., Thompson, A. S., James, C. H., Narayanaswamy, M., and Thurston, D. E. (2009) The pyrrolobenzodiazepine dimer SJG-136 forms sequence-dependent intrastrand DNA cross-links and monoalkylated adducts in addition to interstrand cross-links. *J. Am. Chem. Soc. 131*, 13756–13766.

(24) Mountzouris, J. A., Wang, J.-J., Thurston, D. E., and Hurley, L. H. (1994) Comparison of a DSB-120 DNA interstrand cross-linked adduct with the corresponding bis-tomaymycin adduct: An example of a successful template-directed approach to drug design based upon the monoalkylating compound tomaymycin. *J. Med. Chem. 37*, 3132–3140.

(25) Gait, M. J., Ed. (1984) *Oligonucleotide Synthesis: A Practical Approach*, IRL Press, Oxford, England.

(26) Thompson, A. S., and Hurley, L. H. (1995) Monoalkylation and cross-linking of DNA by cyclopropapyrroloindoles entraps bent and straight forms of A-tracts. *J. Am. Chem. Soc. 117*, 2371–2372.

(27) Sklenar, V., and Bax, A. (1987) Spin echo water suppression for the generation of pure phase two-dimensional NMR spectra. *J. Magn. Reson. 74*, 469–479.

(28) Blake, P. R., and Summers, M. F. (1990) NOESY-1-1-Echo spectroscopy with eliminated radiation damping. *J. Magn. Reson. 86*, 622–624.

(29) Bax, A., Griffey, H., and Hawkins, B. (1983) Correlation of proton and nitrogen-15 chemical shifts by multiple quantum NMR. *J. Magn. Reson. 55*, 301–315.

(30) Purcel, W. P., and Singer, J. A. (1967) Brief review and table of semiempirical parameters used in the Hückel molecular orbital method. *J. Chem. Eng. Data 12*, 235–246.

(31) Gasteiger, J., and Marsili, M. (1980) Iterative partial equalization of orbital electronegativity: A rapid access to atomic charges. *Tetrahedron 36*, 3219–3228.

(32) Young, M. A., Jayaram, B., and Beveridge, D. L. (1997) Intrusion of counterions into the spine of hydration in the minor groove of B-DNA: Fractional occupancy of electronegative pockets. *J. Am. Chem. Soc. 119*, 59–69.

(33) Blanco, M. (1991) Molecular silverware. I. General solutions to excluded volume constrained problems. *J. Comput. Chem. 12*, 237–247.

(34) Hansen, M., and Hurley, L. H. (1995) Altromycin B threads the DNA helix interacting with both the major and the minor grooves to position itself for site-directed alkylation of guanine N7. *J. Am. Chem. Soc. 117*, 2421–2429.

(35) Antonow, D., Barata, T., Jenkins, T. C., Parkinson, D. N., Howard, P. W., Thurston, D. E., and Zloh, M. (2008) Solution structure of a 2:1 C2-(2-naphthyl)pyrrolo[2,1-*c*][1,4]benzodiazepine DNA adduct: Molecular basis for unexpectedly high DNA helix stabilization. *Biochemistry 47*, 11818–11829.

(36) Pettersen, E. F., Goddard, T. D., Huang, C. C., Couch, G. S., Greenblatt, D. M., Meng, E. C., and Ferrin, T. E. (2004) UCSF Chimera: A visualization system for exploratory research and analysis. *J. Comput. Chem. 25*, 1605–1612.

(37) Barkley, M. D., Cheatham, S., Thurston, D. E., and Hurley, L. H. (1986) Pyrrolo[1,4]benzodiazepine antitumour antibiotics: Evidence for two forms of tomaymycin bound to DNA. *Biochemistry 25*, 3021–3031.

(38) Rao, S. N., Singh, U. C., and Kollman, P. A. (1986) Molecular mechanics simulations on covalent complexes between anthramycin and B DNA. *J. Med. Chem. 29*, 2484–2492.

(39) Remers, W. A., Mabilia, M., and Hopfinger, A. J. (1986) Conformations of complexes between pyrrolo[1,4]benzodiazepines and DNA segments. *J. Med. Chem. 29*, 2492–2503.

(40) Zakrzewska, K., and Pullman, B. (1986) A theoretical investigation of the sequence specificity in the binding of the antitumor drug anthramycin to DNA. *J. Biomol. Struct. Dyn. 4*, 127–136.

(41) Krugh, T. R., Graves, D. E., and Stone, M. P. (1989) Two-dimensional NMR studies on the anthramycin-d(ATGCAT)2 adduct. *Biochemistry 28*, 9988–9994.

(42) Patel, D. J. (1982) Antibiotic-DNA interactions: Intermolecular nuclear Overhauser effects in the netropsin-d(CGCGAATTCGCG) complex in solution. *Proc. Natl. Acad. Sci. U.S.A. 79*, 6424–6428.

(43) Graves, D. E., Pattaroni, C., Krishnan, B. S., Ostrander, J. M., Hurley, L. H., and Krugh, T. R. (1984) The reaction of anthramycin with DNA. Proton and carbon nuclear magnetic resonance studies on the structure of the anthramycin-DNA adduct. *J. Biol. Chem. 259*, 8202–8209.

(44) Alley, M. C., Hollingshead, M. G., Pacula-Cox, C. M., Waud, W. R., Hartley, J. A., Howard, P. W., Gregson, S. J., Thurston, D. E., and Sausville, E. A. (2004) SJG-136 (NSC 694501), a novel rationally designed DNA minor groove interstrand cross-linking agent with potent and broad spectrum antitumour activity: Part 2: efficacy evaluations. *Cancer Res. 64*, 6700–6706.

(45) Hartley, J. A., Spanswick, V. J., Brooks, N., Clingen, P. H., McHugh, P. J., Hochhauser, D., Pedley, R. B., Kelland, L. R., Alley, M. C., and Schultz, R. (2004) SJG-136 (NSC 694501), a novel rationally designed DNA minor groove interstrand cross-linking agent with potent and broad spectrum antitumour activity: Part 1: cellular pharmacology, *in vitro* and initial *in vivo* antitumor activity. *Cancer Res. 64*, 6693–6699.

(46) Hartley, J. M., Spanswick, V. J., Gander, M., Giacomini, G., Whelan, J., Souhami, R. L., and Hartley, J. A. (1998) Detection of DNA interstrand crosslinking in clinical samples using the single cell COMET assay. *Ann. Oncol. 9*, 645.

(47) Spanswick, V. J., Hartley, J. M., Ward, T. H., and Hartley, J. A. (2008) Measurement of drug-induced DNA inter-strand cross-linking using the single-cell gel electrophoresis (Comet) assay. *Methods Mol. Med. 28*, 143–154.

(48) Redon, C. E., Nakamura, A. J., Zhang, Y. W., Ji, J. P., Bonner, W. M., Kinders, R. J., Parchment, R. E., Doroshow, J. H., and Pommier, Y. (2010) Histone γH2AX and poly(ADP-ribose) as clinical pharmacodynamic biomarkers. *Clin. Cancer Res. 16*, 4532–4542.